The structure of the Calix[4]arene-(H_2O) cluster, *world's smallest cup of water*

Naoya Hontama[1], Yoshiya Inokuchi[1], Takayuki Ebata[1]*,

Claude Dedonder-Lardeux[2], Christophe Jouvet[2],

and Sotiris S. Xantheas[3]*

[1]Department of Chemistry, Graduate School of Science, Hiroshima University, Higashi-Hiroshima 739-8526, Japan

[2]Laboratoire de Photophysique Moléculaire du CNRS, Bat 210 et Centre Laser de l'Université Paris-Sud, Bat 106, Université Paris-Sud 11, 91405 Orsay, France

[3]Pacific Northwest National Laboratory, 902 Battelle Boulevard, PO Box 999, MS K1-83, Richland, WA 99352, USA

Abstract

The structure of the calix[4]arene(C4A)-(H_2O) cluster formed in a supersonic beam has been investigated by mass-selected resonant two-photon ionization (R2PI) spectroscopy, IR-UV double resonance spectroscopy, IR photodissociation (IRPD) spectroscopy and by high level quantum chemical calculations. The IR-UV double resonance spectrum of C4A-(H_2O) exhibits a broad and strong hydrogen-bonded OH stretching band at 3160 cm^{-1} and a weak asymmetric OH stretching band at 3700 cm^{-1}. The IRPD measurement of the cluster produced a value of 3140 cm^{-1} for the C4A-(H_2O) → C4A + H_2O dissociation energy. High level electronic structure calculations at the MP2 level of theory with basis sets up to quadruple zeta quality suggest that the *endo*-isomer (water inside the C4A cavity) is ~1100 cm^{-1} more stable than the *exo*-isomer (water hydrogen bonded to the rim of C4A). The *endo*-isomer has a best-computed (at the MP2/aug-cc-pVQZ level) value of 3127 cm^{-1} for the binding energy, just ~15 cm^{-1} shy of the experimentally determined threshold and an IR spectrum in excellent agreement with the experimentally observed one. In contrast, the B3LYP density functional fails to even predict a stable structure for the *endo*-isomer demonstrating the inability of that level of theory to describe the delicate balance between structures exhibiting cumulative OH-π H-bonding and dipole-dipole interactions (*endo*-isomer) when compared to the ones emanating from maximizing the cooperative effects associated with the formation of hydrogen bonded homodromic networks (*exo*-isomer). The comparison of the experimental results with the ones from high level electronic structure calculations therefore unambiguously assign the *endo*-isomer as the global minimum of the C4A-(H_2O) cluster, *world's smallest cup of water.*

I. Introduction

Calixarenes (CAs) are cyclic oligomers built with phenol units. They are recognized as molecular receptors and form a variety of complexes with metal ions, anions and neutral molecules.[1-3] CAs have a cavity defined by benzene rings and form *endo*-complexes with hydrophobic molecules and cations through both CH-π and charge-π interactions. In addition, CAs have hydroxyl groups at their lower rim. These OH groups are strongly hydrogen (H)-bonded with each other, resulting in the stabilization of the cone conformation. Although the hydroxyl groups behave as acids, the strong intramolecular H-bonding leads to pKa values for CAs being different from the monomeric units.[4,5] The balance of the interaction between the guest molecule and either the benzene or the hydroxyl group site is very subtle. For example, though it was expected that Calixarenes (C4A) and aliphatic molecules form *endo*-complexes[6] (i.e. the aliphatic molecule lies inside the CA cavity), recent NMR studies revealed that the complex exists as the *exo*-complex having the N^{+}–H---O^{-} form[7,8] (i.e. the aliphatic molecule is located outside the cavity and it is H-bonded to the OH groups).

The complexation structures of CAs are normally studied by NMR and X-ray diffraction methods in the condensed phase,[9-12] whereas mass spectrometric characterization combined with electrospray ionization has been extensively used[13,14] to characterize the gas phase structures. These experimental studies have been carried out at room temperature. Since the thermal energy at these temperatures is oftentimes comparable with the host-guest interaction energy, one generally obtains the information averaged over all possible conformers at a given temperature. In addition, electrospray ionization mass spectrometry generates protonated species, a fact that greatly affects the stabilization of these species. To study a specific complexation

structure of the neutral species controlled by the weak interaction it is essential to cool the complex, and such a study can be performed by the combination of a supersonic jet with laser based spectroscopy. In a previous paper[15] we have reported the first laser spectroscopic study of jet-cooled Calix[4]arene(C4A). We determined the band origin of the S_1-S_0 transition and found that the $S_1(^1A)$ state is strongly vibronically coupled to the $S_2(^1E)$ state. We also showed that C4A has a high ability of forming van der Waals clusters with rare gas atoms.

In the present study we report a joint experimental spectroscopic and theoretical *ab-initio* study of the structure of the C4A-(H_2O) cluster formed in a supersonic beam. Because of the high acidity of the OH groups of C4A, one may expect that water molecule will be exclusively bound to the OH groups to form the *exo*-complex structure. However, it is also quite possible that water is bound inside the C4A cavity by means of OH-π H–bonding interactions. We probe the cluster's structure by measuring the electronic and vibrational spectra and the dissociation energy. The relative energies of the *endo*- and *exo*-conformers of C4A-(H_2O) are estimated from high-level first principles electronic structure calculations and the computed IR spectra for those structures are compared to the experimentally observed one.

II. Approach

Experimental details: In the present work we report the mass-resolved two-color resonance two-photon ionization (2C-R2PI) and IR-UV double resonance spectra of C4A and the C4A-(H_2O) cluster. In addition, we measure the IR photo-dissociation spectrum to obtain the C4A-(H_2O) $\rightarrow$ C4A + H_2O dissociation energy. Fig.1 recaps the basic principles of IR-UV double resonance spectroscopy and IR photo-dissociation

(IRPD) spectroscopy. Briefly, a tunable IR light, ν_{IR}, excites the C4A-(H_2O) cluster in a supersonic beam to the XH stretching vibration, where X refers to either C or O. This IR excitation depletes the population of the ground state. By scanning the IR laser frequency while monitoring the ground state population by R2PI, we obtain the IR-UV dip spectrum (Fig. 1(a)). If the IR photon energy is larger than the dissociation energy of C4A-(H_2O), the cluster dissociates to generate the C4A and H_2O fragments; the C4A fragment can subsequently be monitored by R2PI with the UV laser light, ν_{UV}. By scanning the IR frequency while monitoring the C4A fragment, we obtain the IR photo-dissociation (IRPD) spectrum (Fig. 1(b)). By comparing the IR-UV dip spectrum and the IRPD spectrum, we obtain the dissociation energy (DE) for the process C4A-(H_2O) → C4A + H_2O.

Jet-cooled C4A is generated by an adiabatic expansion of the sample vapor diluted with Ne carrier gas at a total pressure of 2 bars. Since C4A is a nonvolatile molecule, a high temperature pulsed nozzle is used[16]. Briefly, a sample housing made of polyimide resin is attached to the commercially available pulsed nozzle (General valve series 9), and the C4A in the housing is heated at 140 ℃ to obtain enough vapor pressure. For generating the C4A-(H_2O) cluster, a mixture of water vapor and Ne is used as a carrier gas. The gas mixture is expanded into vacuum through the nozzle with a 1mm orifice. The supersonic jet of C4A is then skimmed by a 2 mm aperture skimmer, located at 50 mm downstream of the nozzle. The C4A in the supersonic beam crosses the UV laser and is ionized by R2PI. The ions are extracted into the time-of-flight (TOF) tube, and are detected by a Channeltron (Burle 4900). The TOF profile is monitored by a digital oscilloscope and the ion signals are processed by a boxcar integrator (Stanford research systems SR245) connected to a personal computer. The

tunable UV laser is a second harmonic (Inrad Auto-tracker III/BBO crystal) of Nd:YAG laser pumped dye laser (Continuum Surelite II/Lambda Physique Scanmate). For the two-color R2PI (2C-R2PI) experiment, the third harmonic of another Nd:YAG laser is used for the ionization step. The delay time between the first laser and the second laser is fixed to a few nanoseconds. Details of the IR-UV dip spectroscopy were given in previous papers. A UV probe laser is fixed to the 0-0 band of the monitored species and a tunable IR laser (Laser Vision/Quanta-Ray, GCR250) light is introduced coaxially to the UV probe laser 110 ns prior to the probe pulse. IRPD spectrum is obtained with the same setup, except that the C4A fragment mass is monitored and the UV laser frequency is fixed to its transition. C4A (98%) was purchased from Tokyo Chemical Industry Co. and was used without further purification.

Theoretical calculations: The relative energies of the *endo*- and *exo*- isomers of the C4A-(H_2O) cluster are optimized at the second order Moller-Plesset (MP2) level of theory[17] with the family of augmented correlation consistent basis sets of Dunning and co-workers[18,19] up to quadruple-zeta quality, aug-cc-pV*n*Z (*n* = D, T, Q). The MP2/aug-cc-pVDZ optimal geometries were used for single point calculations with the larger basis sets of Dunning up to aug-cc-pVQZ. These calculations were performed with the NWChem suite of electronic structure codes[20] at Pacific Northwest National Laboratory. The MP2 relative energetics are compared to the ones from density functional theory (DFT) calculations with the B3LYP functional and the 6-31+G** basis set[21] with the GAUSSIAN 03 program package.[22]. The harmonic vibrational frequencies were estimated at the MP2/aug-cc-pVDZ level of theory for both isomers and they were scaled by 0.96 in order to produce the IR spectra that are compared to

experiment.

The binding energy of the C4A-(H_2O) cluster is computed as:

$$\Delta E(C4A-H_2O) = E^{C4A-H_2O}_{C4A-H_2O}(C4A-H_2O) - E^{C4A}_{C4A}(C4A) - E^{H_2O}_{H_2O}(H_2O) \qquad (1)$$

, where superscripts denote basis sets and subscripts indicate the geometries of the individual species identified in parentheses. In this notation, for example, $E^{C4A}_{C4A-H_2O}(C4A)$ denotes the energy of C4A at the dimer (C4A-H_2O) geometry with the monomer (C4A) basis set.

The basis set superposition error (BSSE) correction was estimated via the function counterpoise (fCP) method[23] including the fragment relaxation terms[24], which arise from the change in the intramolecular geometry of the C4A and H_2O fragments in the cluster minimum. The BSSE-corrected dimer binding energies are:

$$\begin{aligned}\Delta E_{BSSE}(C4A-H_2O) &= E^{C4A-H_2O}_{C4A-H_2O}(C4A-H_2O) - E^{C4A-H_2O}_{C4A-H_2O}(C4A) - E^{C4A-H_2O}_{C4A-H_2O}(H_2O) \\ &+ E^{C4A}_{rel}(C4A) + E^{H_2O}_{rel}(H_2O)\end{aligned} \qquad (2)$$

and

$$E^{C4A}_{rel}(C4A) = E^{C4A}_{C4A-H_2O}(C4A) - E^{C4A}_{C4A}(C4A) \qquad (3a)$$

$$E^{H_2O}_{rel}(H_2O) = E^{H_2O}_{C4A-H_2O}(H_2O) - E^{H_2O}_{H_2O}(H_2O). \qquad (3b)$$

A total of 4 additional calculations (C4A and H_2O with the full cluster basis at the cluster and isolated MP2/aug-cc-pVDZ geometries) are therefore required for each BSSE calculation.

III. Results and discussion

S_1-S_0 electronic spectra

Figure 2 shows the 2C-R2PI spectra of (a) C4A, (b) C4A-Ar and (c) C4A-(H_2O) generated in a supersonic beam. The spectrum of bare C4A exhibits a band origin at

35357 cm^{-1} and sharp intense bands at ~ 170 cm^{-1} above the band origin. The electronic spectrum of C4A-Ar is very similar to that of the bare C4A, except that all the bands are red-shifted by 45 cm^{-1} with respect to those of C4A. The C4A-Ar cluster is an *endo*-complex, in which the Ar atom is located inside the C4A cavity, retaining overall C_4 symmetry.[25] In contrast, the spectrum of C4A-(H_2O) is quite different from that of either C4A or C4A-Ar. First, the band origin is red-shifted by ~200 cm^{-1} from that of the bare C4A and the vibronic structure is quite complicated. A weak band at 35151 cm^{-1}, located at the lowest frequency side, is thought to be the origin band and several low frequency vibronic bands emerge. The strong vibronic bands at ~35340 cm^{-1} (0,0 + 190 cm^{-1}) are broad, a fact that may be due to the overlap of several bands. The complicated structure of the 0,0 band indicates that the cluster does not have C_4 symmetry and the structure largely changes upon the electronic excitation.

IR-UV double resonance and IRPD spectra

Figures 3(a) and (b) show the IR-UV double resonance (DR) spectra of the bare C4A and the C4A-(H_2O) cluster, respectively. The IR-UV DR spectrum of C4A exhibits a strong and broad OH stretching band centered at 3160 cm^{-1}. This band is red-shifted by as much as 500 cm^{-1} from the frequency of the free OH stretch of phenol which is at 3657 cm^{-1}. The weak band at 3040 cm^{-1} is assigned to the CH stretching vibration of the aromatic ring. In the IR-UV DR spectrum of C4A-(H_2O) a strong H-bonded OH stretch band also emerges at 3160 cm^{-1}. The position of this band is the same with that of bare C4A (cf. Fig. 3(a)), but its bandwidth is wider and a few peaks seem to be overlapped within this band. The fact that the OH stretching frequency of the C4A-(H_2O) cluster is the same with that of bare C4A, indicates that the OH groups of

the C4A moiety are not affected by the complexation with water, that is the water molecule is not bound to the OH groups. In addition to the strong band at 3160 cm^{-1}, the IR-UV DR spectrum exhibits a weak band at 3700 cm^{-1}, which is assigned to the asymmetric (free) OH stretching vibration of H_2O.

Figure 3 (e) shows the IRPD spectrum of the C4A-(H_2O) cluster. The spectrum is obtained by scanning the IR laser frequency while monitoring the $C4A^+$ cation mass with the UV frequency fixed near the band origin of C4A. When comparing the IRPD with the IR-UV dip spectrum, we observe a sharp cutoff at 3140 $\pm$ 20 cm^{-1} in the IRPD spectrum and below this energy the C4A fragment is not detected even though the C4A-(H_2O) cluster has an IR absorption in that range. Thus, this threshold energy (3140 $\pm$ 20 cm^{-1}) corresponds to the C4A-$(H_2O)_1$ $\rightarrow$ C4A + H_2O dissociation energy.

The structure of the C4A-(H_2O) cluster

In order to determine the lowest energy structure of the C4A-(H_2O) cluster we performed initial optimizations at the B3LYP/6-31+G** level of theory. These calculations yielded four *exo*-conformers (whose structures are shown in the Supporting Information), but failed to yield a stable *endo*-isomer structure. In contrast, the MP2/aug-cc-pVDZ optimizations did produce a stable *endo*-isomer structure, which was determined to be the global minimum (*vide infra*). The minimum energy structures of the most stable among the *exo*-conformers (Structure I) and the global minimum *endo*-isomer (Structure II) of the C4A-(H_2O) cluster obtained at the MP2/aug-cc-pVDZ level of theory are shown in Figure 4. The relative energies, ΔE_{endo} and ΔE_{exo}, of the *endo*- and *exo*-isomers (in cm^{-1}) and their relative separation, $\Delta\Delta E=(\Delta E_{endo}-\Delta E_{exo})$ are listed in Table 1 at the MP2 level of theory with the

aug-cc-pV*n*Z, *n*=D. T, Q basis sets together with the relaxation energies for the C4A and water (obtained from equations 3(a) and 3(b)). These are the energy penalties for distorting the geometries of the two moieties (C4A and water) from their gas phase structures to the ones they assume in the C4A-(H_2O) cluster. The BSSE-corrected isomer binding energies (calculated from equation (2)) are also shown in parentheses. We note that the *endo*-isomer is always more stable (with any of the aug-cc-pV*n*Z, *n*=D, T, Q basis sets) than the *exo*-isomer. Furthermore, the energy separation between the two isomers converges with basis set to about 1100 cm^{-1}, the *endo*-isomer being more stable. As expected from the observation of the optimal geometries shown in Fig. 4, the C4A moiety is much more distorted in the *exo*- than in the *endo*-isomers, whereas the distortion of the water molecule in both isomers is minimal, as indicated from the magnitude of the relaxation energies for the two moieties listed in Table 1. Finally the best computed (MP2/aug-cc-pVQZ) binding energy of 3127 cm^{-1} of the most stable *endo*-isomer is in excellent agreement with the experimentally determined threshold of 3140 $\pm$ 20 cm^{-1}. The variation of the uncorrected and BSSE-corrected binding energies listed in Table 1 suggests that the MP2/aug-cc-pVQZ energy is probably an upper limit for the binding energy of the *endo*-isomer.

In the *exo*-isomer (Structure I) the water molecule is inserted into and enlarges the ring homodromic network originally formed by the four OH groups of C4A. The resulting five OH homodromic ring is consistent with the network having the largest cooperativity[26]. In this structure, the H-bonding network of the OH groups in C4A is largely distorted by the insertion of the water molecule by ca. 2000 cm^{-1} as reported in Table 1. As a result, in the calculated IR spectrum of *exo*-isomer (Structure I), the degenerated OH stretching bands in the C4A moiety are split in the wide energy region

as indicated in Fig. 3(d).

In contrast, the IR spectrum of the most stable *endo*-isomer (Structure II) is much more simpler, attesting to the minimal (~100 cm^{-1}) distortion of the C4A moiety in the C4A-(H_2O) complex. In the observed IR spectrum of the *endo*-isomer (shown in Fig. 3(b)), there is no band between 3250 and 3650 cm^{-1}. This spectral pattern is consistent with the theoretically calculated IR spectrum at the MP2/aug-cc-pVDZ level of theory. The calculated IR spectrum of "Structure II" (Fig. 3(c)) shows a perfect agreement with the observed one (Fig. 3(b)). The degenerate OH stretching bands of C4A at 3160 cm^{-1} are split into two due to the symmetry reduction since the encapsulation of the water molecule lowers the symmetry of C4A. This is the reason why the observed band at 3160 cm^{-1} is broader than that of bare C4A. The band at 3700 cm^{-1} is the asymetirc OH stretch of the encapsulated water, which also reproduces the observed spectrum quite well. In the *endo*-isomer (Structure II) the two OH groups of the water molecule are bound to two phenyl rings in a bidentate manner and the oxygen atom of the water molecule is facing towards the rim of C4A. The reason for this arrangement can be thought of originating from the dipole-dipole interactions between C4A and the water molecule. The dipole moment of C4A is 2.37 Debye, oriented along the C_4 axis and pointing in a downward direction towards the rim. Thus, the oxygen atom of the water molecule in the cavity prefers to be oriented towards the rim of C4A in order to maximize the dipole-dipole interaction between the two fragments. The synergy between the two OH-π H-bonding and dipole-dipole interactions results in the large stabilization energy of "Structure II" with respect to the H-bonded homodromic *exo*-isomer (Structure I).

The combination of the above findings, namely that (*i)* the *endo*-isomer is

lower in energy at the MP2 level of theory, (*ii*) its best estimate for the binding energy matches within 15 cm^{-1} the experimentally determined threshold for the dissociation energy of the cluster into the C4A and water fragments and (*iii*) the computed IR spectra of the *endo*-isomer shows a perfect agreement with the experimentally observed ones makes the unambiguous assignment that the observed structure corresponds to the *endo*-isomer of the C4A-(H_2O) cluster, in which the water molecule resides within the C4A cavity.

IV. Conclusions

The structure of the C4A-(H_2O) cluster offers the possibility to probe the delicate balance between the cumulative OH-π H-bonding and dipole-dipole interactions on one hand and the maximization of the cooperative effects associated with the formation of H-bonded homodromic networks on the other. The structure of this cluster has been probed by IR-UV double resonance spectroscopy, IRPD spectroscopy and high level electronic structure calculations. The IR-UV spectrum exhibits a broad and strong H-bonded OH stretch band at 3160 cm^{-1} and an asymmetric OH stretch at 3700 cm^{-1}, whereas the IRPD measurement yields the H-bond energy to be 3140 cm^{-1}. High level electronic structure calculations at the MP2 level of theory with basis sets as large as aug-cc-pVQZ suggest that the minimum structure resembles an *endo*-complex. The best computed (MP2/aug-cc-pVQZ) binding energy for that isomer is 3127 cm^{-1}, in excellent agreement with the experimentally determined threshold of 3140 cm^{-1}. In addition, the MP2/aug-cc-pVDZ calculated IR spectrum of the *endo*-isomer showed excellent agreement with the experimentally observed one. It is interesting to note that the B3LYP functional with the 6-31+G** basis set fails to

produce a stable minimum for that structure, incorrectly predicting the *exo*-isomer as the most stable one; however, neither the binding energy (estimated at 1100 cm^{-1} higher than that for the *endo*-isomer at the MP2 level of theory) nor the computed IR spectrum for that structure matches the experiment.

In the most stable *endo*-isomer the two OH groups of the water molecule are bound to the phenyl rings via OH—π bonding and the need to maximize the dipole-dipole interactions orients the water molecule in such a way that its oxygen faces towards the rim of the C4A, thus forming "*the smallest cup of water in the world*".

Acknowledgements:

Part of this work is supported by JSPS and MAE under the Japanese-France Integrated Action Program (SAKURA). T. E. also acknowledges JSPS for the support through a Grant-in-Aid project (No. 18205003) and MEXT for the support through a Grant-in-Aid for the Scientific Research on Priority Area "Molecular Science for Supra Functional Systems" (No. 477). Part of this work is supported by the Chemical Sciences, Geosciences and Biosciences Division, Office of Basic Energy Sciences, US Department of Energy. Battelle operates the Pacific Northwest National Laboratory for the U.S. Department of Energy. This research was performed in part using the Molecular Science Computing Facility (MSCF) in the Environmental Molecular Sciences Laboratory, a national scientific user facility sponsored by the Department of Energy's Office of Biological and Environmental Research.

References

1. Gutsche, C. D. “Calixarenes”, in *Monographss in Supramolucular Chemistry*, ed. Stoddart, J. F. Royal Society of Chemistry, Cambridge, **1989.**
2. Cram, D. J.; Cram, J. M. “Container molecules and their guests”, in *Monographss in Supramolucular Chemistry*, ed. Stoddart, J. F. Royal Society of Chemistry, **1994.**
3. Gutsche, C. D. “Calixarenes revisited”, in *Monographss in Supramolucular Chemistry*, ed. Stoddart, J. F. Royal Society of Chemistry, Cambridge, **1998.**
4. Araki, K.; Iwamoto, K.; Shinkai, S.; Matsuda, T. *Bull. Chem. Soc. Jpn.* **1990**, *63*, 3480.
5. Cunningham, I. D.; Woodfall, M. *J. Org. Chem.* **2005** , 70 , 9248
6. Gutsche, C. D.; Bauer, L. *J. Am. Chem. Soc.* **1985**, 107, 6063.
7. Nachtigall, F. F.; Lazzarottoa, M.; Nome, F. *J. Braz. Chem. Soc.* **2002**, 13, 295
8. Puchta, R.; Clark, T.; Bauer, W. *J. Mol. Model,* **2006**, 12, 739
9. Benevelli, F.; Kolodziejski, W.; Wozniak, K.; Klinowski, J. *Chem. Phys. Lett.* **1999**, 308, 65
10. Molins, M. A.; Nieto, P. M.; Sanchez, C.; Prados, P.; Mendoza, J. De; Pons, M. *J. Org. Chem.* **1992**, 57, 6924
11. Buscemi, S.; Pace, A.; Piccionello, A. P.; Pappalardo, S.; Garozo, D.; Pilati, T.; Gattuso, G.; Pappalardo, A.; Pisagatti, I.; Parisi, M. F.; *Tetrahed. Lett.* **2006**, 47, 9049
12. Kuzmicz, R.; Dobrzycki, L.; Wozniak, K.; Benevelli, F.; Klinowski, J.; Kolodziejski, W. *Phys. Chem. Chem. Phys.* **2002**, 4, 2387
13. Schalley, C. A.; Castellano, R. K.; Brody, M. S.; Rudkevich, D. M.; Siuzdak, G.; Rebek, J. Jr. *J. Am. Chem. Soc.* **1999**,121, 4568

14. Zadmard, R.; Kraft, A.; Schrader, T.; Linne, W. *Chem.-A Europ. J.* **2004**, 10, 4233

15. Ebata, T.; Hodono, Y.; Ito, T.; Inokuchi, Y. *J. Chem. Phys.* **2007**, 126, 141101

16. Ebata, T. *Bull. Chem. Soc. Jpn.* **2009**, 82, 127.

17. Møller, C.; Plesset, M. S., *Phys. Rev.* **1934**, *46,* 618

18. Dunning Jr., T. H., *J. Chem. Phys.* **1989**, *90,* 1007;

19. Kendall, R. A.; Dunning Jr., T. H.; Harrison, R. J.; *J. Chem. Phys.* **1992**, *96,* 6796

20. Kendall R. A.; Aprà, E.; Bernholdt, D. E.; Bylaska, E. J.; Dupuis. M.; Fann, G. I.; Harrison, R. J.; Ju., J.; Nichols, J. A.; Nieplocha, J.; Straatsma, T. P.; Windus, T. L.; Wong, A. T.; *Comp. Phys. Comm*. **2000**, 128: 260-283; High Performance Computational Chemistry Group (2003) NWChem, A Computational Chemistry Package for Parallel Computers, Version 4.6. Pacific Northwest National Laboratory, Richland, Washington 99352, USA

21. Hehre, W. J.; Ditchfield, R.; Pople, J. A.; *J. Chem. Phys*. **1972**, 56: 2257

22. Frisch, M. J.; Trucks, G. W.; Schlegel, H. B.; Scuseria, G. E.; Robb, M. A.; Cheeseman, J. R.; Montgomery Jr., J. A.; Vreven, T.; Kudin, K. N.; Burant, J. C.; Millam, J. M. ; Iyengar, S. S. ; Tomasi, J. ; Barone, V. ; Mennucci, B. ; Cossi, M. ; Scalmani, G.; Rega, N.; Petersson, G. A.; Nakatsuji, H.; Hada, M.; Ehara, M.; Toyota, K.; Fukuda, R.; Hasegawa, J.; Ishida, M.; Nakajima, T.; Honda, Y.; Kitao, O.; Nakai, H.; Klene, M.; Li, X.; Knox, J. E.; Hratchian, H. P.; Cross, J. B.; Adamo, C.; Jaramillo, J.; Gomperts, R.; Stratmann, R. E.; Yazyev, O.; Austin, A. J.; Cammi, R.; Pomelli, C.; Ochterski, J. W.; Ayala, P. Y.; Morokuma, K; Voth, G. A.; Salvador, P.; Dannenberg, J. J.; Zakrzewski, V. G.; Dapprich, S.; Daniels, A. D.; Strain, M. C.; Farkas, O.; Malick, D. K.; Rabuck, A. D.; Raghavachari, K.; Foresman, J. B.; Ortiz, J. V.; Cui, Q.; Baboul, A. G.; Clifford, S.; Cioslowski, J.; Stefanov, B. B.; Liu,

G.; Liashenko, A.; Piskorz, P.; Komaromi, I.; Martin, R. L.; Fox, D. J.; Keith, T.; Al-Laham, M. A.; Peng, C. Y.; Nanayakkara, A.; Challacombe, M.; Gill, P. M. W.; Johnson, B.; Chen, W.; Wong, M. W.; Gonzalez, C.; Pople, J. A. *Gaussian, Inc., Pittsburgh PA*, **2003**.

23. Boys, S. F.; Bernardi, F.; *Mol. Phys.* **1970**, *19*, 553
24. Xantheas, S. S.; *J. Chem. Phys.* **1996**, *104*, 8821
25. Ebata, T.; Hontama, N.; Inokuchi, Y.; Haino, T.; Xantheas, S. S. ; (in preparation)
26. Xantheas, S. S.; *Chem. Phys.* **2000**, *258*, 225

Table 1. Total binding (ΔE_{endo}, ΔE_{exo}) and relative ($\Delta\Delta E=\Delta E_{endo}-\Delta E_{exo}$) energies (in cm^{-1}) of the global minimum *endo*- and the local minimum *exo*-isomers of the C4A-(H_2O) cluster. Numbers in parentheses indicate BSSE-corrected numbers. The relaxation energies for C4A and water (distortion of the C4A and water moieties in the cluster from their gas phase structures) are also denoted for the two isomers.

Level of theory	*Endo*-form ΔE_{endo}, cm^{-1}	E_{relax} cm^{-1}	*Exo*-form ΔE_{exo}, cm^{-1}	E_{relax} cm^{-1}	$\Delta\Delta E$ cm^{-1}
MP2/aug-cc-pVDZ	4312 (2455)	121 / 11	2561 (1349)	2009 / 57	1751 (1106)
MP2/aug-cc-pVTZ	3602 (2789)	81 / 34	2228 (1687)	2004 / 86	1374 (1102)
MP2/aug-cc-pVQZ	3127		1985		1142

Figure captions

Figure 1. Left panel: Energy level diagram of C4A and C4A-(H_2O) and IR-UV excitation schemes. Right panel: (a) IR –UV dip spectrum and (b) IRPD spectrum.

Figure 2. 2C-R2PI spectra of (a) C4A, (b) C4A-Ar and (c) C4A-(H_2O).

Figure 3. IR-UV dip spectra of (a) C4A and (b) C4A-(H_2O). IR spectra of (c) *endo*-(Structure II) and (d) *exo*-form of C4A-(H_2O) (Structure I) obtained at the MP2/aug-cc-pVDZ level of theory. The frequencies are multiplied by 0.96. (e) IRPD spectrum of C4A-(H_2O).

Figure 4. (a) Minimum energy structures of the *exo*- (Structure I) and *endo*-conformers (Structure II) of the C4A-(H_2O) cluster obtained at the MP2/aug-cc-pVDZ level of theory.

Fig. 1 Hontama et al.

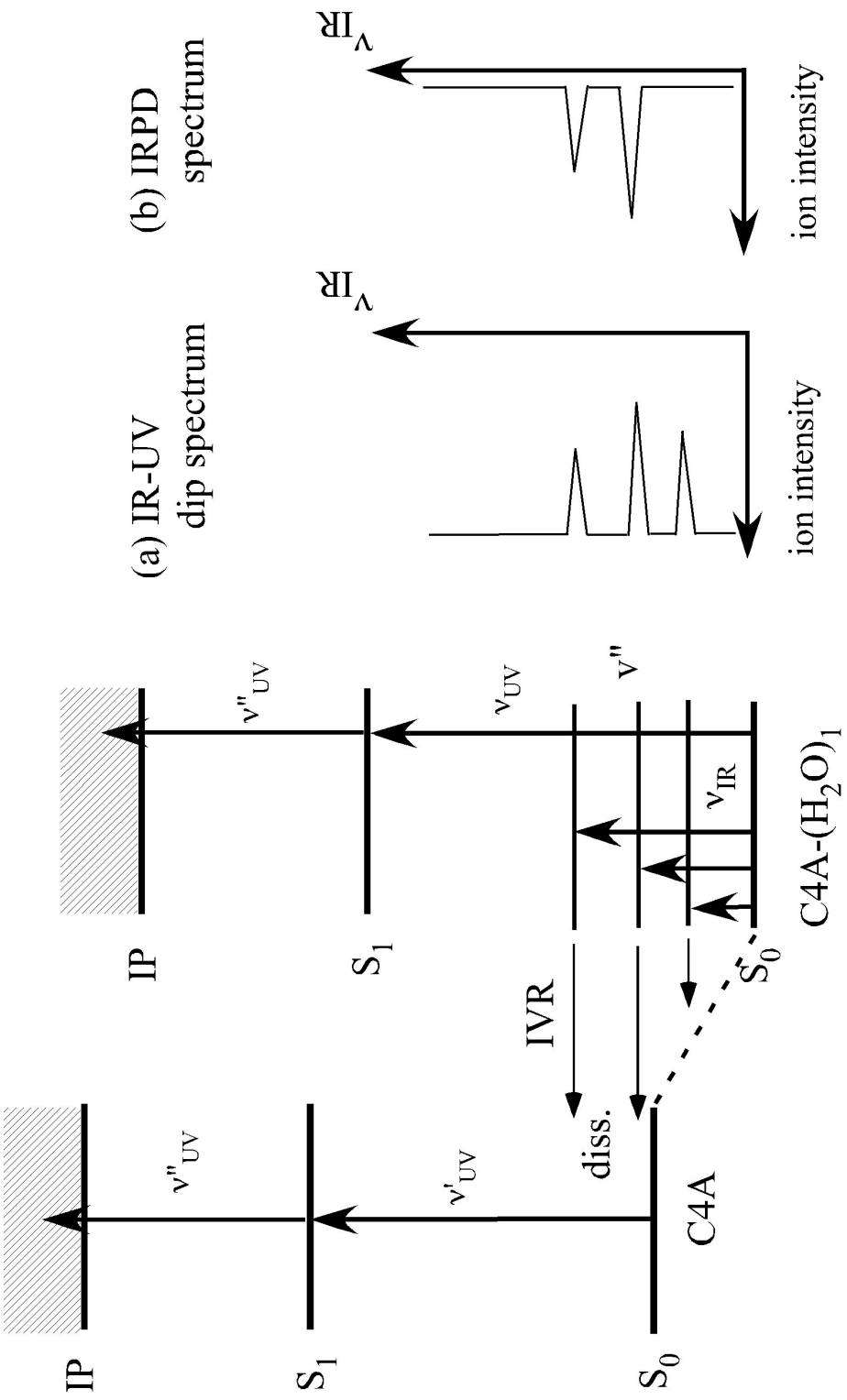

Fig. 2 Hontama et al.

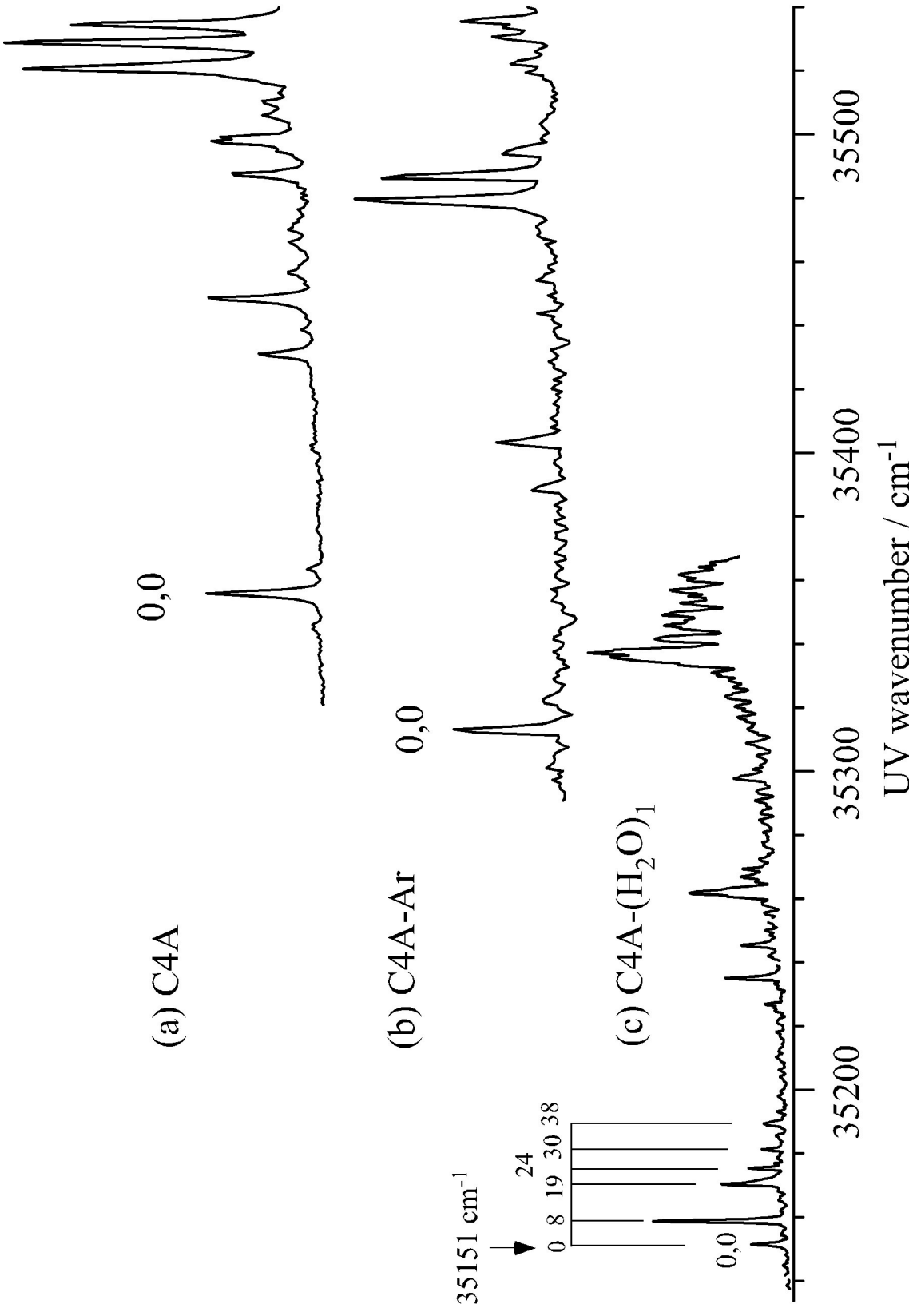

Fig. 3 Hontama et al.

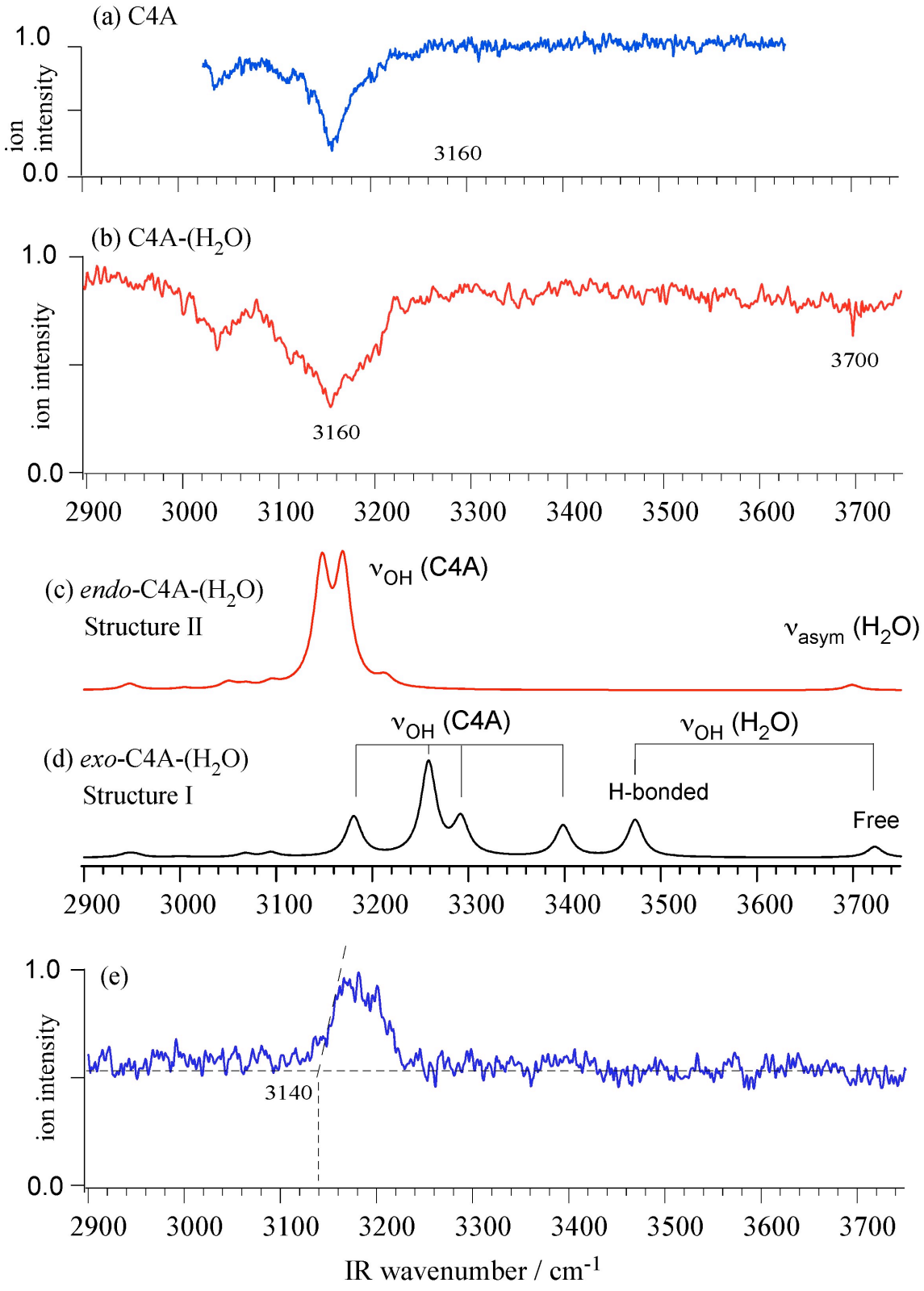

Fig. 4 Hontama et al.

(a) Structure I *exo*- C4A-(H_2O)

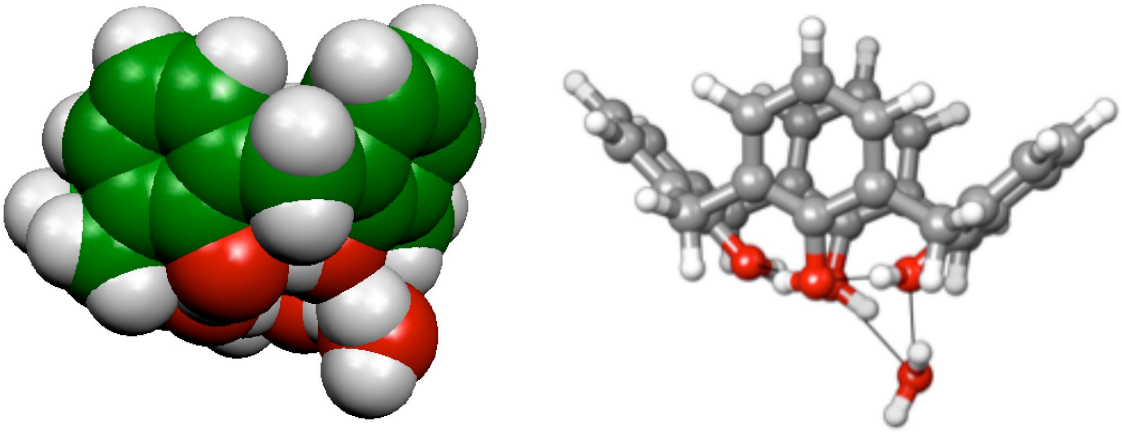

+1100 cm^{-1}

(b) Structure II *endo*- C4A-(H_2O)

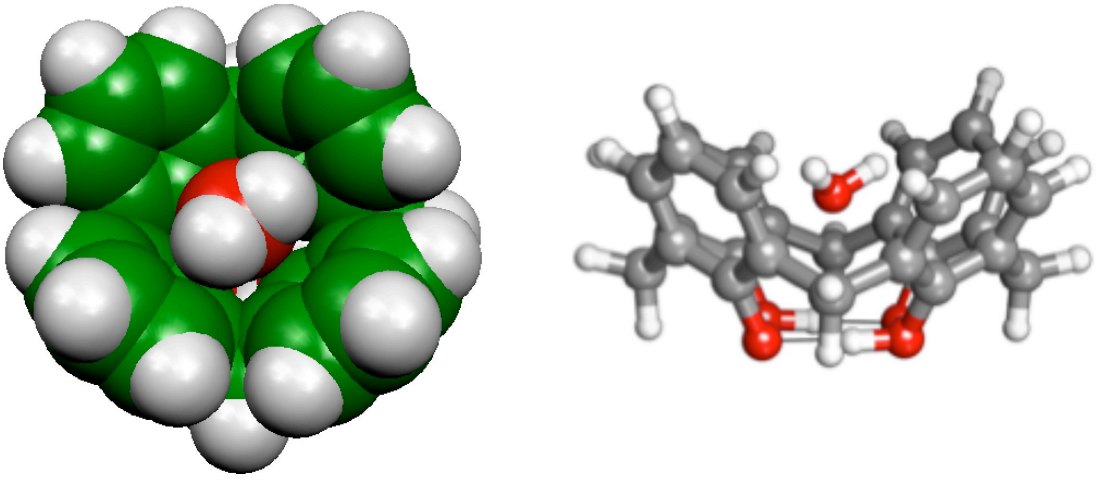

+0 cm^{-1}

Supporting information

Optimized structures and relative energies of the various *exo*-conformers of the C4A-(H_2O) cluster obtained at B3LYP/6-31+G** level of theory.